Received: 24 October 2023 | Revised: 15 April 2024 | Accepted: 17 April 2024

DOI: 10.1111/mpp.13464

Molecular Plant Pathology | WILEY

ORIGINAL ARTICLE

An effector SsCVNH promotes the virulence of *Sclerotinia sclerotiorum* through targeting class III peroxidase AtPRX71

Ming Ma[1,2] | Liguang Tang[3] | Rui Sun[1,2] | Xueliang Lyu[1,2] | Jiatao Xie[1,2] | Yanping Fu[2] | Bo Li[1,2] | Tao Chen[1,2] | Yang Lin[2] | Xiao Yu[1,2] | Weidong Chen[4] | Daohong Jiang[1,2] | Jiasen Cheng[1,2]

[1]National Key Laboratory of Agricultural Microbiology, Huazhong Agricultural University, Wuhan, Hubei, China

[2]The Provincial Key Lab of Plant Pathology of Hubei Province, College of Plant Science and Technology, Huazhong Agricultural University, Wuhan, Hubei, China

[3]Wuhan Vegetable Research Institute, Wuhan Academy of Agricultural Science, Wuhan, Hubei, China

[4]United States Department of Agriculture, Agricultural Research Service, Washington State University, Pullman, Washington, USA

Correspondence
Jiasen Cheng, National Key Laboratory of Agricultural Microbiology, Huazhong Agricultural University, Wuhan 430070, Hubei, China.
Email: jiasencheng@mail.hzau.edu.cn

Funding information
National Natural Science Foundation of China, Grant/Award Number: 31701735, 32172368 and 32130087; The earmarked fund of China Agriculture Research System, Grant/Award Number: CARS-12; Huazhong Agricultural University Scientific and Technological Self-innovation Foundation, Grant/Award Number: 2021ZKPY014

Abstract

Many plant pathogens secrete effector proteins into the host plant to suppress host immunity and facilitate pathogen colonization. The necrotrophic pathogen *Sclerotinia sclerotiorum* causes severe plant diseases and results in enormous economic losses, in which secreted proteins play a crucial role. SsCVNH was previously reported as a secreted protein, and its expression is significantly upregulated at 3 h after inoculation on the host plant. Here, we further demonstrated that deletion of *SsCVNH* leads to attenuated virulence. Heterologous expression of *SsCVNH* in *Arabidopsis* enhanced pathogen infection, inhibited the host PAMP-triggered immunity (PTI) response and increased plant susceptibility to *S. sclerotiorum*. SsCVNH interacted with class III peroxidase AtPRX71, a positive regulator of innate immunity against plant pathogens. SsCVNH could also interact with other class III peroxidases, thus reducing peroxidase activity and suppressing plant immunity. Our results reveal a new infection strategy employed by *S. sclerotiorum* in which the fungus suppresses the function of class III peroxidases, the major component of PTI to promote its own infection.

KEYWORDS
AtPRX71, peroxidase, *Sclerotinia sclerotiorum*, SsCVNH

1 | INTRODUCTION

Sclerotinia sclerotiorum is a ubiquitous and destructive necrotrophic fungus (Boland & Hall, 1994; Bolton et al., 2006; Purdy, 1979). It has about 425 plant species as hosts and causes the symptoms of leaf maceration and Sclerotinia stem rot (SSR) (Derbyshire et al., 2022). To survive in adverse environments, *S. sclerotiorum* can form black sclerotia, which are capable of surviving in the soil for up to 10 years (Adams & Ayers, 1979). Under suitable conditions, sclerotia can germinate by means of mycelium or carpogenically by producing

apothecia to release ascospores, both of which can infect host plants (Clarkson et al., 2007). There are no cultivars with high resistance that can be used in production (Zhao et al., 2009). Although new fungicides are continually being developed to prevent Sclerotinia diseases, the frequency of fungicide-resistant strains of *S. sclerotiorum* in the field is increasing (Duan et al., 2018, 2019; Tao et al., 2021). Sclerotinia disease is highly challenging to control and causes huge economic losses annually.

Plants have evolved two major layers of innate immune system: PAMP (pathogen-associated molecular pattern)-triggered immunity (PTI) and effector-triggered immunity (ETI) (Couto & Zipfel, 2016; Jones & Dangl, 2006). PTI is an early defence response triggered by molecular patterns, which are recognized by pattern recognition receptors (PRRs) on the cell membrane (Boutrot & Zipfel, 2017; Jones & Dangl, 2006; Macho & Zipfel, 2014). PRR activation events mainly consist of ion fluxes, oxidative burst, activation of mitogen-activated protein kinases (MAPKs), changes in protein phosphorylation, ethylene biosynthesis, receptor endocytosis, gene activation and callose deposition (Ausubel, 2005; Boller & Felix, 2009; Qi et al., 2022). Reactive oxygen species (ROS) act as signalling molecules and by-products of aerobic metabolism (Mittler et al., 2011). Following pathogen attack, oxidative burst is one of the fastest defence responses to be activated (Yu et al., 2017). ROS play a critical role in plant resistance against pathogens. There are three primary types of enzymes involved in ROS scavenging (superoxide dismutase, catalase and peroxidase) and two main types of enzymes involved in ROS production (respiratory burst oxidase and peroxidase) (Jia et al., 2013; Waszczak et al., 2018; Yu et al., 2017). The roles of plant peroxidases in ROS are complex. Peroxidases are a huge family; some members (AT3G49110 and AT3G49120) participate in ROS production, and some members (Os05g04470 and Os10g39170) participate in ROS scavenging (Daudi et al., 2012; Li et al., 2017). Based on their structure and catalytic properties, peroxidases can be divided into three superfamilies. The first and second peroxidase superfamilies consist of animal peroxidases and catalases, respectively (Hiraga et al., 2001). Because of the difference in primary structure, the third peroxidase superfamily is further divided into three classes (I, II and III) (Cosio & Dunand, 2009; Hiraga et al., 2001). Class I peroxidases also split further into three groups: ascorbate peroxidases (APxs), bacterial catalase–peroxidases (CPs) and cytochrome c peroxidases (CcPs) (Hiraga et al., 2001). APxs are mainly localized in the chloroplast, peroxisome and cytoplasm (Cosio & Dunand, 2009; Teixeira et al., 2004). CcPs localize in the mitochondrial intermembrane space. Class II peroxidases are encoded by fungi and play a major role in the degradation of soil debris. Class III peroxidases are secreted glycoproteins encoded by a large multigene family in plants (Bakalovic et al., 2006; Cosio & Dunand, 2009; Gara, 2004; Hiraga et al., 2001; Jia et al., 2013). Class III peroxidase gene *OsPrx30* contributes to the bacterial blight *Xanthomonas oryzae* pv. *oryzae* infection by promoting peroxidase activity and reducing the levels of hydrogen peroxide (Liu et al., 2020).

As a typical necrotrophic fungus, much research on the pathogenesis of *S. sclerotiorum* focuses on oxalic acid (OA) and cell wall-degrading enzymes (CWDEs). OA suppresses the host defence response, including callose deposition and autophagy, promotes plant programmed cell death (PCD) and reduces ambient pH (Godoy et al., 1990; Gómez-Gómez & Boller, 2000; Kabbage et al., 2013; Kim et al., 2008; Marolano et al., 1983). Moreover, OA also induces increased levels of ROS and subsequently triggers programmed cell death. This process is essential for the virulence of *S. sclerotiorum*, indicating that ROS play a significant role in the interaction between host plants and *S. sclerotiorum* (Kim et al., 2008). To cope with oxidative stress during infection, *S. sclerotiorum* activates its antioxidant defences. For example, at high levels of host-derived ROS, the expression levels of three copper ion import/transport genes *Ssctr1*, *Sscc*s and *Ssatx1*, all of which are involved in fungal ROS detoxification and virulence, are markedly upregulated during infection (Ding et al., 2020). A mutant of Cu/Zn superoxide dismutase (SOD) also exhibits increased sensitivity to oxidative stress in culture and reduced ability to detoxify superoxide in infected leaves, and its virulence also decreased accordingly (Xu & Chen, 2013). Interestingly, although *S. sclerotiorum* is a necrotrophic fungal pathogen, there is a short biotrophic interaction between plants and *S. sclerotiorum* (Kabbage et al., 2013, 2015). So, there is a two-phase infection model in which the pathogen first evades, counteracts and subverts the host's basal defence reactions prior to killing and degrading host cells (Liang & Rollins, 2018). It reflects the complexity of the pathogenesis of *S. sclerotiorum*.

Several studies have shown that secreted proteins play an important role in the infection process of *S. sclerotiorum*. Genomic analysis showed that there are 879 genes encoding secreted proteins in *S. sclerotiorum* (Amselem et al., 2011). Transcriptomic analysis revealed that many genes encoding secreted proteins are upregulated during infection in different host plants (tomato, *Nicotiana benthamiana* and *Arabidopsis thaliana*) in *S. sclerotiorum*, and some of them have been identified as candidate effectors (Gupta et al., 2022; Guyon et al., 2014; Lyu et al., 2015). Peyraud revealed that a total of 1133 genes were induced to upregulate expression when *S. sclerotiorum* was inoculated on *A. thaliana* or on solid medium in vitro (Peyraud et al., 2019). Up to now, a few effectors have been studied in the pathogenesis of *S. sclerotiorum*. For example, SsITL suppresses host resistance by targeting the calcium-sensing receptor CAS in chloroplasts (Tang et al., 2020; Zhu et al., 2013). SsCaf1 is not only required for infection cushion formation but can also trigger cell death when expressed in tobacco (Xiao et al., 2014). SsSSVP1 interacts with QCR8, a subunit of the cytochrome b-c1 complex, to disturb the localization of QCR8 in mitochondria, thereby facilitating the infection of *S. sclerotiorum* (Lyu et al., 2016). SsCP1 targets pathogenesis-related protein PR1 directly and contributes to the virulence of *S. sclerotiorum* (Yang et al., 2017). The PGIP-INactivating Effector 1 (SsPINE1) directly interacts with and functionally inactivates polygalacturonase-inhibiting proteins (PGIPs) and then suppresses plant immunity and promotes infection in *S. sclerotiorum* (Wei et al., 2022). Effector protein SsERP1 (ethylene pathway repressor protein 1) participates in the pathogenesis of *S. sclerotiorum* and

promotes infection by inhibiting the plant ethylene signalling pathway (Fan et al., 2021). In the late stage of *S. sclerotiorum* infection, SsXyl2, a glycosyl hydrolase family 11 xylanase, is secreted to promote cell necrosis by targeting NbHIR2 on the plasma membrane (Wang et al., 2024). These studies indicate that secreted proteins are involved in the pathogenesis of *S. sclerotiorum*. However, there are more secreted proteins whose functions and mechanisms still need to be elucidated.

In a previous study, we found that a secreted protein *S. sclerotiorum* cyanovirin-N homologue (SsCVNH) plays an important role in the pathogenesis of *S. sclerotiorum*, and silencing of *SsCVNH* significantly decreased the virulence of *S. sclerotiorum* (Lyu et al., 2015). We demonstrated that SsCVNH targeted the class III peroxidase superfamily in plants, which is associated with ROS production and acts as a positive regulator of innate immunity against fungi and bacteria (Daudi et al., 2012; Lorrai et al., 2021; Raggi et al., 2015; Zhao et al., 2019). SsCVNH interfered with ROS homeostasis, reduced peroxidase activity and decreased the activation of defence gene transcription, thereby contributing to the virulence of *S. sclerotiorum*. Our findings not only extend our knowledge of the mechanisms of secreted proteins in the pathogenesis of *S. sclerotiorum*, but also deepen our understanding of the role of ROS in *Sclerotinia*–plant interaction.

2 | RESULTS

2.1 | *SsCVNH* plays a crucial role in virulence of *S. sclerotiorum*

We previously reported that a small, cysteine-rich secretory protein called SsCVNH was dramatically induced during infection, and the virulence of *S. sclerotiorum* was significantly reduced in SsCVNH-silenced transformants (Lyu et al., 2015). However, the specific role of SsCVNH in the pathogenesis and the underlying mechanisms has not been elucidated. To further clarify the function of SsCVNH, three *SsCVNH* knockout mutants (Δ*SsCVNH1*, Δ*SsCVNH4* and Δ*SsCVNH6*) were generated through homologous recombination (Figure S1a). The complemented strains (Δ*SsCVNH4*-C2 and Δ*SsCVNH4*-C3) were generated by introducing the wild-type allele into Δ*SsCVNH4* using *Agrobacterium tumefaciens*-mediated transformation (ATMT) (Figure S1b–f). Results showed that the virulence of Δ*SsCVNH* mutants was significantly reduced. Whether inoculated onto oilseed rape or *A. thaliana*, the lesions produced by Δ*SsCVNH* mutants were all obviously (33.5%–47.4%) smaller than that caused by the wild-type strain (Figure 1). The virulence of two complemented strains (Δ*SsCVNH4*-C2 and Δ*SsCVNH4*-C3) was restored to the wild-type level (Figure 1). However, there was no significant difference between the Δ*SsCVNH* mutants and the wild-type strain 1980 in terms of colony morphology, growth rate, sclerotial development, oxalic acid production and infection cushion formation (Figure 2), indicating SsCVNH was not essential for normal growth and development. These results demonstrated that SsCVNH was indeed an important virulence factor in *S. sclerotiorum*.

2.2 | SsCVNH suppresses plant immune responses

Considering that SsCVNH is a secreted protein, to study its effects on plants, stable *Arabidopsis* transgenic plants constitutively expressing *SsCVNH* driven by the cauliflower mosaic virus 35S promoter were generated in the wild-type Columbia-0 (Col-0) genetic background. Two independent lines, 35S:*SsCVNH-6* and 35S:*SsCVNH-27*, were selected for further study through reverse transcription (RT)-PCR and western blot assays (Figure S2a,b). Plants of these two *SsCVNH*-overexpressing lines showed morphology and growth similar to the wild-type Col-0 (Figure S2c). In addition, we found that SsCVNH might exist in a variety of monomeric, dimeric and trimeric forms in plants (Figure S2b). Then, the plant immune responses were characterized. As an early response, the accumulation of chitin-triggered or NEP2-triggered ROS in *SsCVNH*-overexpressing plants was noticeably lower compared to that in Col-0 (Figures 3a and S2d). The chitin-induced callose deposition was significantly (50%–59%) lower in *SsCVNH*-overexpressing plants (Figure 3b,c). In addition, the resistance-associated genes *GST6*, *PR1*, *FRK1* and *NHL10* showed lower induction upon chitin treatment (Figure 3d). Consistent with these results, *SsCVNH*-overexpressing plants exhibited more severe and faster disease symptoms, with a necrotic area of 21.9%–29.9% bigger than that of wild-type plants (Figure 3e,f). Taken together, our data suggested that overexpression of SsCVNH inhibited the plant immune response and increased susceptibility of plants to *S. sclerotiorum*.

2.3 | SsCVNH interacts with a class III peroxidase AtPRX71 in the cell membrane and apoplast

In order to identify the target proteins of SsCVNH in plants, we used a cDNA library of *A. thaliana* infected by *S. sclerotiorum* in yeast two-hybrid (Y2H) screening. SsCVNH could be expressed normally in Y2HGold, and no self-activation phenomenon was observed (Figure S3). After screening the *Arabidopsis* cDNA library, 71 plant proteins were identified as potential interacting proteins (Table S1). Eleven proteins were confirmed to interact with SsCVNH in the Y2H assay (Figure S4). Among these 11 target proteins, PSBO2 (AT3G50820), AtPRX71 (AT5G64120) and a protein with unknown function (AT5G47030) interacted with SsCVNH several times in the screening (12, 6 and 5 times, respectively) (Figures 4a and S4). Among the 71 potential interacting proteins, AtTHI1, AtIGMT4 and AtMKK2 did not interact with SsCVNH (Figure 4a). Based on the fact that AtPRX71 was the only one among the three proteins reported to be related to plant defence response, it was selected for further study. To investigate the interaction between SsCVNH and AtPRX71 in plants, we transiently co-expressed AtPRX71-cRFP (C-terminal red fluorescent protein

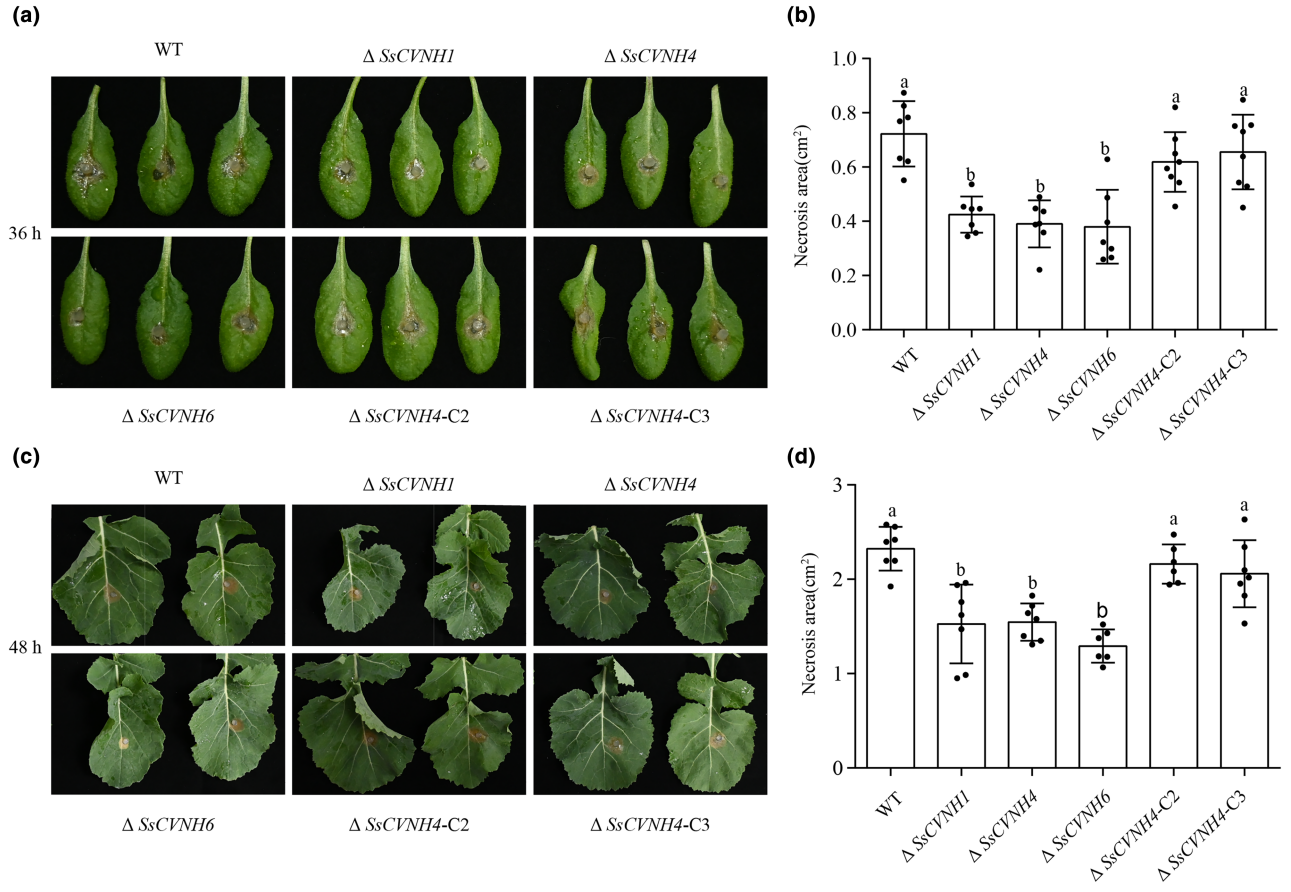

FIGURE 1 *SsCVNH* plays a crucial role in virulence of *Sclerotinia sclerotiorum*. (a) Disease symptoms on 5-week-old detached *Arabidopsis thaliana* Col-0 leaves caused by wild-type strain 1980 (WT), three deletion mutants Δ*SsCVNH1*, Δ*SsCVNH4*, Δ*SsCVNH6*) and two complemented strains (Δ*SsCVNH4*-C2 and Δ*SsCVNH4*-C3). Representative leaves are shown and photographed at 36 h post-inoculation (hpi). (b) Lesion area means ± *SD* and were analysed by one-way analysis of variance (ANOVA) ($p < 0.05$). (c) Disease symptoms on detached *Brassica napus* leaves caused by wild-type strain 1980, the three deletion mutants and two complemented strains. Representative leaves are shown and photographed at 48 hpi. (d) Lesion area means ± *SD* by one-way ANOVA ($p < 0.05$). Three times independent replicates were carried out, and each strain was inoculated with seven Col-0 leaves. Different lowercase above bars indicate significant difference.

fragment) and SsCVNH-nRFP (N-terminal red fluorescent protein fragment) in *N. benthamiana* leaves. As shown in Figure 4b, red fluorescence was observed, indicating that SsCVNH interacted with AtPRX71 in plant cells. Furthermore, this interaction was confirmed using a co-immunoprecipitation (Co-IP) assay (Figure 4c). The results showed that SsCVNH was indeed associated with AtPRX71 in planta. These results indicated that SsCVNH physically interacts with AtPRX71.

To determine the subcellular localization of SsCVNH, we transiently expressed SsCVNH-GFP, SsCVNH$^{\Delta SP}$-GFP and GFP proteins in 4-week-old leaves of *N. benthamiana*. Fluorescence analysis showed that full-length SsCVNH with signal peptide (SP) was localized in the cell membrane, whereas SsCVNH$^{\Delta SP}$ had the same localization as GFP in the cytoplasm (Figure 5a). However, AtPRX71 is known to localize in the extracellular region rather than the cell membrane (Raggi et al., 2015). Thus, total proteins and apoplast proteins were extracted after transiently expressing SsCVNH-FLAG and SsCVNH$^{\Delta SP}$-FLAG in *N. benthamiana*. The immunoblotting analysis showed that SsCVNH-FLAG was detected in both the apoplast proteins and the total proteins, while SsCVNH$^{\Delta SP}$-FLAG was only detected in the total proteins (Figure 5b). Subsequently, AtPRX71-GFP and SsCVNH-mCherry were transiently co-expressed in *N. benthamiana*, and a complete yellow fluorescence was observed on the cell membrane after overlapping the GFP and RFP signals (Figure 5c). These results suggest that SsCVNH functions by interacting with AtPRX71 in the cell membranes and apoplast in *N. benthamiana* plants.

2.4 | AtPRX71 positively modulates plant immunity

Stable 35S:*AtPRX71*-GFP-overexpressing *Arabidopsis* Col-0 lines were created to investigate the functions of AtPRX71 in plant immunity. Two transgenic lines, 35S:*AtPRX71-7* and 35S:*AtPRX71-9*, with high expression levels in western blot validation were selected for further study (Figure S5a). A T-DNA insertion mutant, *Atprx71* (SALK_061054C), was also confirmed to be homozygous at the

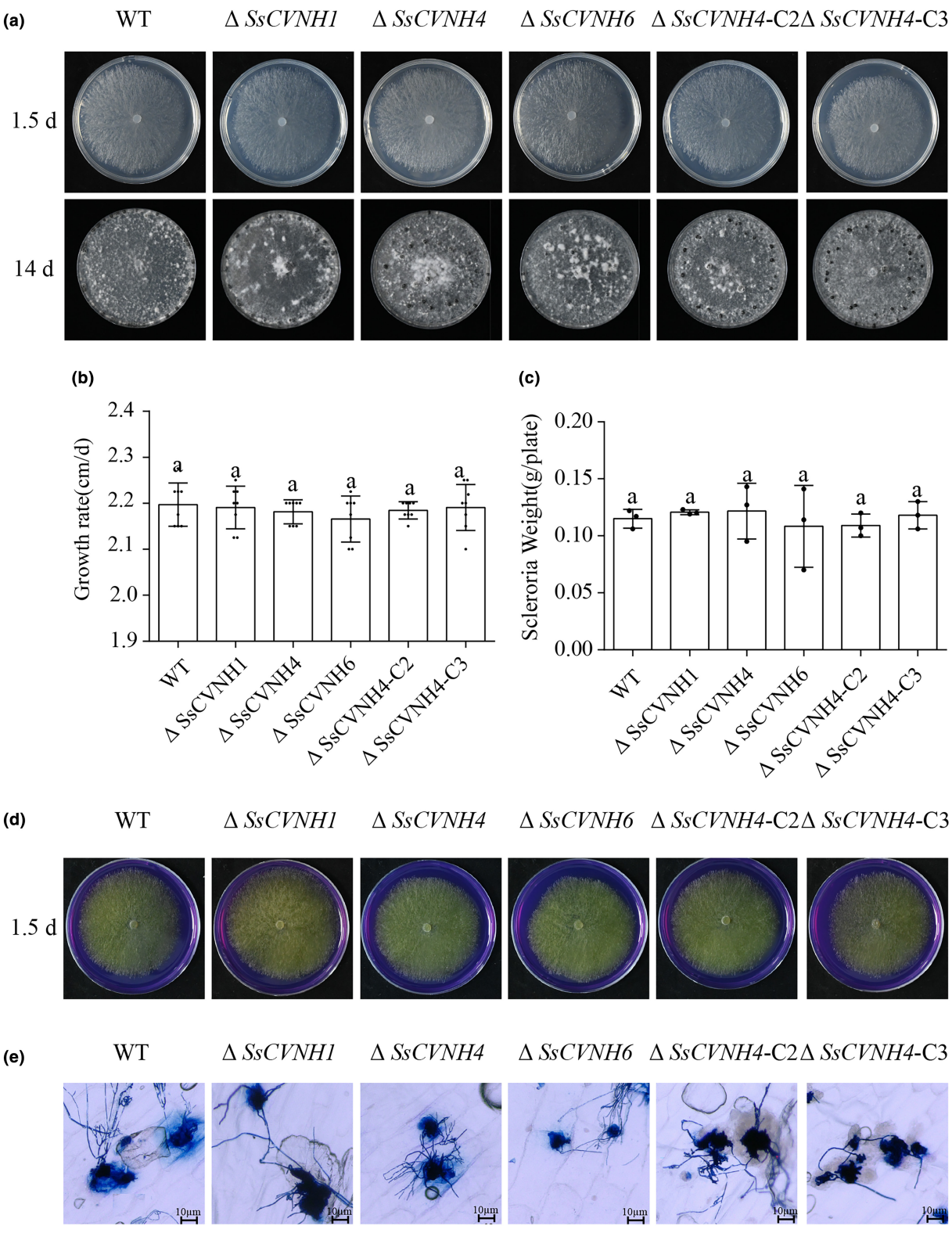

FIGURE 2 *SsCVNH* deletion had no effect on morphology and normal saprophytic growth. (a) Colony morphology and sclerotial development of wild-type (WT), Δ*SsCVNH1*, Δ*SsCVNH4*, Δ*SsCVNH6*, Δ*SsCVNH4*-C2 and Δ*SsCVNH4*-C3 on potato dextrose agar (PDA) at 20°C, photographed at 1.5 days and 14 days. (b) Growth rate of above strains on PDA at 20°C. (c) Sclerotial weight per plate of different strains. Data represent means ± *SD*. Different lowercase letters above bars indicate significant difference. (d) Detection of oxalate production on PDA containing 0.005% (wt/vol) bromophenol blue dye by WT, Δ*SsCVNH1*, Δ*SsCVNH4*, Δ*SsCVNH6*, Δ*SsCVNH4*-C2 and Δ*SsCVNH4*-C3, photographed at 36 h after inoculation. The yellow region indicated that oxalic acid was produced. (e) Infection cushion formation of WT, the three deletion mutants and two complemented strains at 14 h after inoculation on onion leaves and stained with trypan blue. The pictures were photographed by ultra-depth-of-field microscope. Scale bars = 10 μm.

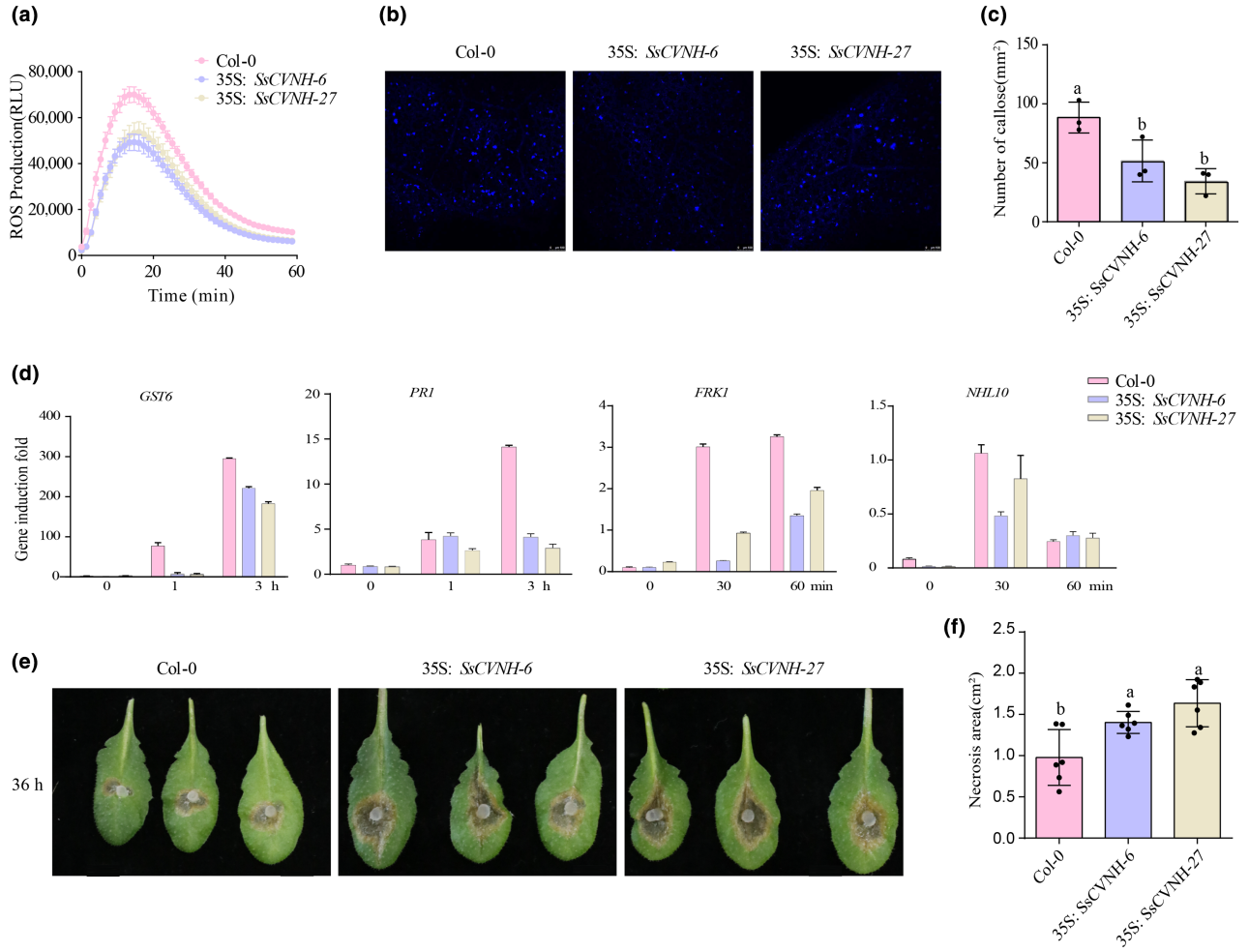

FIGURE 3 SsCVNH suppresses the host immune response. (a) Comparison of chitin-induced reactive oxygen species (ROS) burst of *SsCVNH*-overexpressing *Arabidopsis* lines with the wild-type Col-0. Leaf discs from 5-week-old plants (35S:*SsCVNH-6*, 35S:*SsCVNH-27* and Col-0) were treated with 200 nM chitin for 60 min, and the relative light emission was measured. Values represent means ± *SEM* ($n = 14$). (b) Compromised chitin-induced callose deposition in 35S:*SsCVNH* transgenic lines. Five-week-old plants were infiltrated with 500 nM chitin and stained with aniline blue. Scale bars = 100 μm. (c) Quantification of callose using ImageJ software. Values represent the means ± *SD* ($n = 9$), and they were analysed by a one-way analysis of variance (ANOVA). Different lowercase letters above bars indicate significant difference. (d) Induction of disease resistance-related genes in 5-week-old 35S:*SsCVNH* transgenic lines and Col-0 plants at 0, 1 and 3 h or 0, 30 and 60 min, after treating with 200 nM chitin. Total RNA was extracted, and data were normalized to the expression of *AtPGADH* in reverse transcription quantitative PCR analysis. (e) Disease symptoms on detached leaves of 5-week-old 35S:*SsCVNH-6*, 35S:*SsCVNH-27* and Col-0 plants inoculated with *Sclerotinia sclerotiorum* wild-type strain 1980. Photographs were taken at 36 h post-inoculation. The experiments were performed at least three times with at least six *Arabidopsis* leaves. (f) Histogram comparing the necrosis areas on 35S:*SsCVNH-6*, 35S:*SsCVNH-27* and Col-0 plants. Values represent the means ± *SD* ($n = 6$) by one-way ANOVA. Different lowercase letters above bars indicate significant difference.

insertion locus by PCR (Figure S5b). Compared with the wild-type Col-0, there were no significant differences in growth and morphology of the *AtPRX71*-overexpressing lines and the *Atprx71* mutant (Figure S5c).

Then, the different *A. thaliana* lines were tested for their response to chitin. Results showed that compared with Col-0, 35S:*AtPRX71-7* and 35S:*AtPRX71-9* showed significantly increased levels of chitin-induced ROS burst. Conversely, the chitin-triggered ROS production was markedly inhibited in the *Atprx71* mutant (Figure 6a). Subsequently, callose deposition, another hallmark of plant immunity, was detected after chitin treatment. We found that callose deposition in overexpressing lines 35S:*AtPRX71-7* and 35S:*AtPRX71-9* increased by 67.9% and 76.9%, respectively, compared with Col-0. However, there was no significant difference between the *Atprx71* mutant and Col-0 (Figure 6b,c). After inoculation with *S. sclerotiorum*, the lesion areas were 32.9%–44.8% smaller in 35S:*AtPRX71*-overexpressing plants than in Col-0 plants at 36 h post-infiltration (hpi), and there was no significant difference in the lesion areas between the *Atprx71* mutant and Col-0 (Figure 6d,e). For example, the lesion areas were only 0.49 and 0.36 cm^2 on 35S:*AtPRX71-7* and 35S:*AtPRX71-9* plants, but 1.11 cm^2 on the leaves of Col-0 and *Atprx71* mutant plants. This indicates that AtPRX71 positively enhances plant resistance to *S. sclerotiorum* (Figure 6d,e). Collectively, these data demonstrate that AtPRX71 could act as a

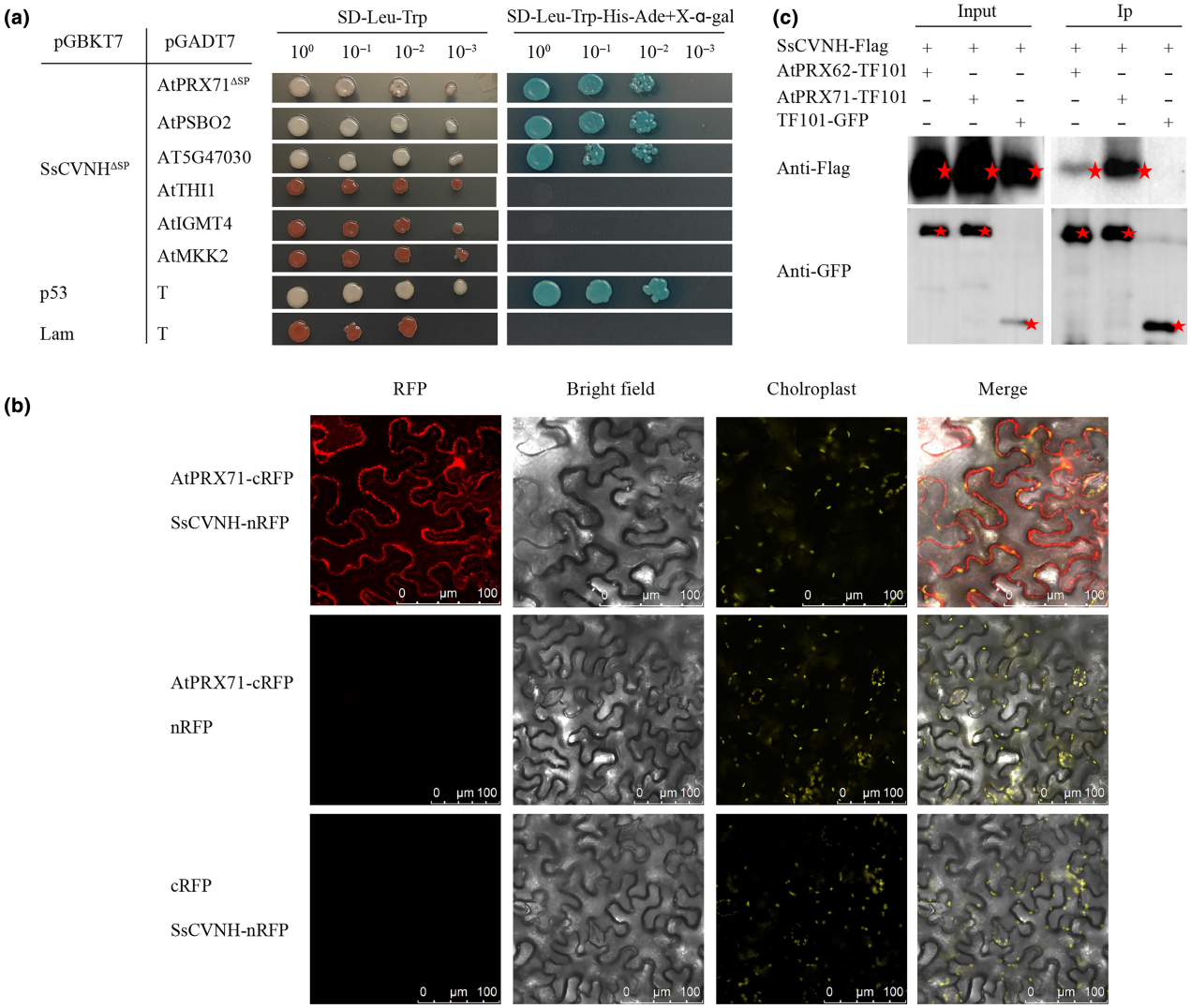

FIGURE 4 SsCVNH physically interacts with a class III peroxidase AtPRX71 in the cell membrane and apoplast. (a) Yeast two-hybrid assay verified that PSBO2 (AT3G50820), AtPRX71 (AT5G64120) and AT5G47030 interacted with SsCVNH, while AtTHI1, AtIGMT4 and AtMKK2 could not. (b) Bimolecular fluorescence complementation assay confirms the in vivo interaction of SsCVNH with AtPRX71. Co-expressing of SsCVNH-nRFP and AtPRX71-cRFP or negative controls nRFP and AtPRX71-cRFP or SsCVNH-nRFP and cRFP. The fluorescence of mCherry was monitored at 2 days post-agroinfiltration using confocal laser scanning microscopy. Scale bars = 100 μm. (c) Co-immunoprecipitation confirms the in planta association of SsCVNH and AtPRX71. SsCVNH-FLAG was expressed in *Nicotiana benthamiana* together with AtPRXs-TF101-GFP or TF101-GFP. Immunoprecipitation was performed with anti-GFP antibody coupled to GFP trap, followed by western blotting. Input, immunoblots of total proteins using anti-GFP and anti-FLAG antibodies; IP, after washing with washing buffer, proteins were added to 1 × SDS loading buffer and then detected using anti-GFP and anti-FLAG antibodies.

positive regulatory factor to enhance plant immunity and resistance to pathogen invasion.

2.5 | SsCVNH inhibits ROS burst through interaction with AtPRX71 and its superfamily

AtPRX71 belongs to the class III superfamily, which contains a conserved peroxidase domain (Raggi et al., 2015). The class III superfamily has 73 members, including nine peroxidases (AtPRX2, AtPRX25, AtPRX33, AtPRX34, AtPRX37, AtPRX43, AtPRX52, AtPRX62 and AtPRX69). These nine peroxidases were selected to verify their interaction with SsCVNH using the luciferase complementation assay (LCA). We observed different strengths of luciferase (LUC) signals when SsCVNH$^{\Delta SP}$-nLUC and AtPRXs$^{\Delta SP}$-cLUC or SsCVNH$^{\Delta SP}$-nLUC and AtAPX1-cLUC were co-expressed in *N. benthamiana* leaves. This indicates that SsCVNH interacts with these nine peroxidases in addition to AtPRX71 (Figure 7a). Consistent with the LCA results, the Y2H assay result also indicated that SsCVNH could interact with all 10 members (Figure 7b). These results were further confirmed by co-expressing SsCVNH-mCherry with AtPRX34-GFP or AtPRX62-GFP in *N. benthamiana*. The co-localization of SsCVNH with AtPRX34 and AtPRX62 was observed in the membrane and extracellular space (Figure 7c). All

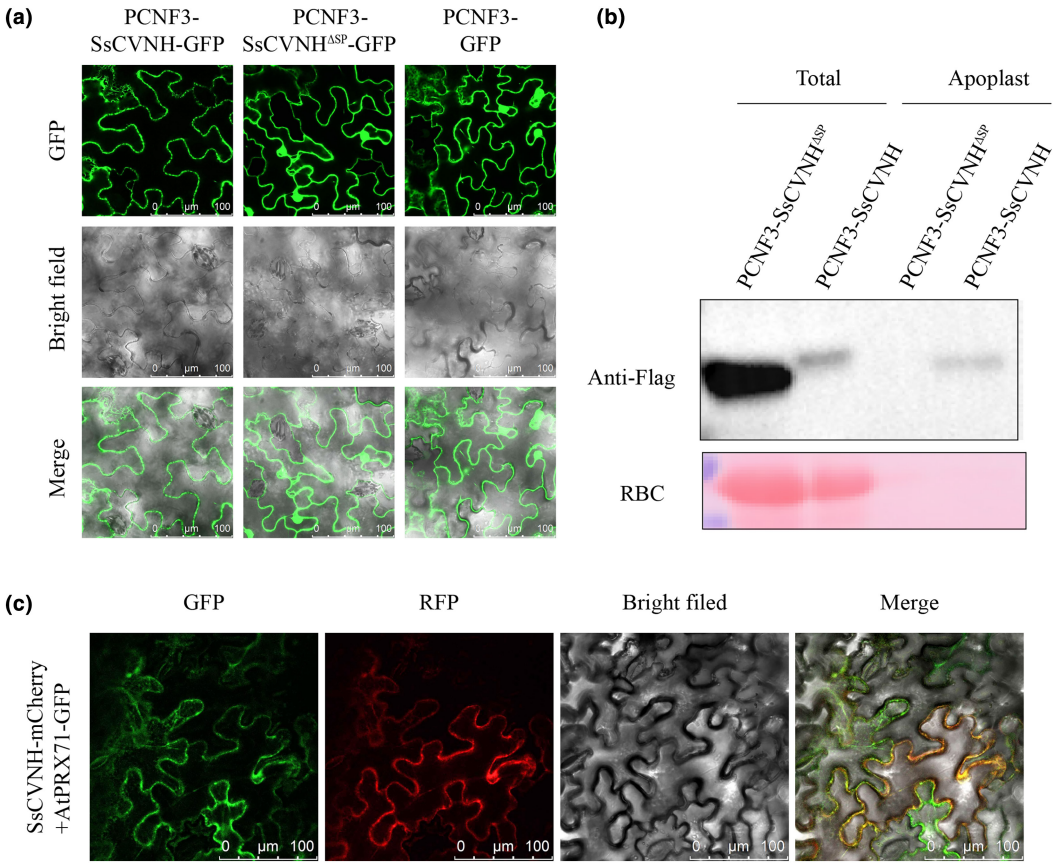

FIGURE 5 Subcellular localization of SsCVNH in plants. (a) Confocal images showing SsCVNH$^{\Delta SP}$-GFP fusion protein distributed in the cytoplasm and SsCVNH-GFP fusion protein localized in the cell membrane. Fluorescence (GFP) and bright field confocal images were acquired 2 days after agroinfiltration. Scale bars = 100 μm. (b) Western blot analysis of proteins in apoplast fluids and total cell extract after transiently expressing SsCVNH-FLAG and SsCVNH$^{\Delta SP}$-FLAG in *Nicotiana benthamiana* epidermal cells. Ponceau S staining was used to evaluate the protein loading of RuBisCO (RBC). (c) Subcellular localization after co-expressing SsCVNH-mCherry with AtPRX71-GFP in the *N. benthamiana* epidermal cells; the photographs were taken 3 days after agroinfiltration using confocal laser scanning microscopy. Scale bars = 100 μm.

the findings indicate that SsCVNH targets all these members of the peroxidase class III superfamily.

To determine the specific region of SsCVNH that interacted with AtPRX71, we generated three truncated SsCVNH mutant variants: SsCVNH1 (21–101 amino acids [aa]), SsCVNH2 (61–145 aa) and SsCVNH3 (101–153 aa). These variants were then tested using the Y2H assay (Figure 8a). The Y2H results showed that the truncated SsCVNH1 and SsCVNH2 mutants without SP could interact with AtPRX71 but SsCVNH3 without SP could not, suggesting that the region 61–101 of SsCVNH was likely to be important for the interaction between SsCVNH and AtPRX71 (Figure 8b). Interestingly, the full-length SsCVNH inhibited chitin-induced ROS bursts, while SP-removed SsCVNH did not. These results indicated that the correct location of SsCVNH is important for its function. Furthermore, when SsCVNH1 and SsCVNH2 were fused with a SP, it was also able to inhibit the ROS burst induced by chitin. However, SsCVNH3, which does not interact with AtPRX71, lost its ability to inhibit ROS burst after being fused with a SP. This suggests that the interaction between SsCVNH and AtPRX71 is necessary for SsCVNH to effectively inhibit the plant immune response (Figure 8c). These results indicated that the region 61–101 of SsCVNH is required and sufficient for interaction with AtPRX71 and function in suppressing chitin-induced ROS. In plants, high peroxidase activity results in high production of ROS, which plays a crucial role in plant disease resistance (Raggi et al., 2015), and we found that the activity of peroxidase enzymes in 35S:*SsCVNH* transgenic lines was significantly inhibited, suggesting that SsCVNH may affect the function of AtPRXs through the physical interaction (Figure 8d).

3 | DISCUSSION

S. sclerotiorum can produce a large arsenal of secreted proteins, some of which act as CWDEs to promote infection and colonization or act as PAMPs to induce plant immune responses or act as effectors to promote the invasion and disrupt host immune response (Lyu et al., 2015, 2016; Yang et al., 2022, 2023). In this study, we demonstrated that SsCVNH, an important virulence effector, can reduce the host's ROS levels, making the host susceptible to *S. sclerotiorum* by targeting peroxidases.

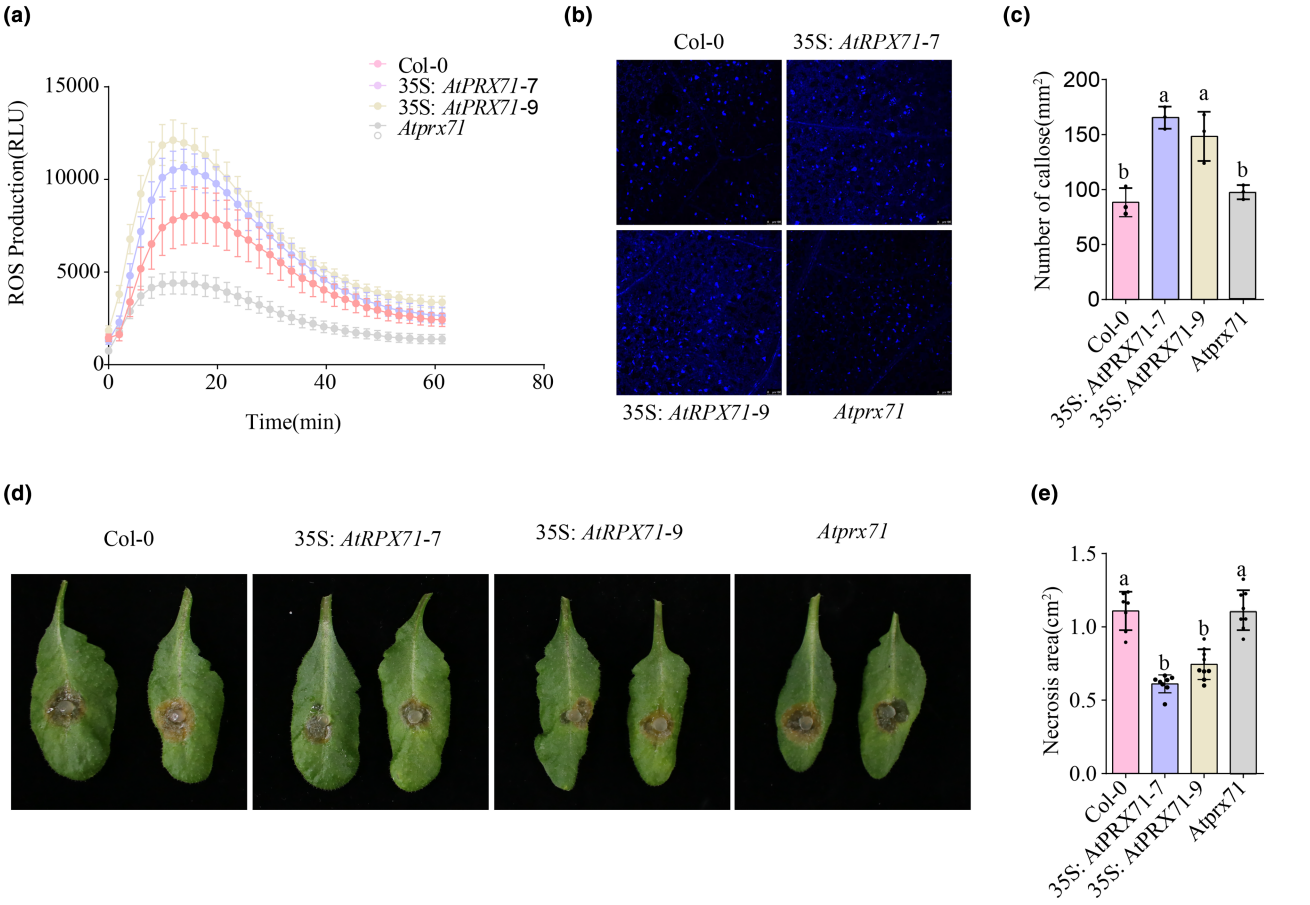

FIGURE 6 AtPRX71 positively modulated plant immunity. (a) 35S:*AtPRX71*-overexpressing lines promoted chitin-induced reactive oxygen species (ROS) burst. Leaf discs from 5-week-old plants (35S:*AtPRX71-7*, 35S:*AtPRX71-9*, *Atprx71* and Col-0) were treated with 200 nM chitin, and the relative light emissions were measured. Values represent means ± *SEM* ($n = 18$). (b) Callose deposition in 35S:*AtPRX71-7*, 35S:*AtPRX71-9*, *Atprx71* mutant lines and Col-0 was detected. Five-week-old plants were infiltrated with 500 nM chitin and stained with aniline blue. Scale bars = 100 μm. (c) Quantification of chitin-induced callose deposition in 35S:*AtPRX71*-overexpressing lines using ImageJ. Values represent the means ± *SD* ($n = 9$), and they were analysed by one-way analysis of variance (ANOVA). Different lowercase letters above bars indicate significant difference. (d) Disease symptoms caused by wild-type strain *Sclerotinia sclerotiorum* on detached leaves of 5-week-old 35S:*AtPRX71-7*, 35S:*AtPRX71-9*, *Atprx71* and Col-0 plants. Photographs were taken at 36 h post-inoculation. (e) Histogram comparing the necrosis areas. Values represent the means ± *SD* ($n = 7$) by one-way ANOVA. The experiments were performed at least three times. Different lowercase letters above bars indicate significant difference.

In our earlier study, *SsCVNH* showed the greatest increase in gene expression during infection of *A. thaliana* leaves (Lyu et al., 2015). The CVNH domain mainly exists in cyanobacteria, filamentous ascomycetes (just *Sclerotinia* and *Botryotinia*) and *Ceratopteris richardii* (Percudani et al., 2005). The predicted three-dimensional structure of SsCVNH is extremely similar to the protein structure of cyanovirin-N (CV-N) in the cyanobacterium *Nostoc ellipsosporum* (Barrientos et al., 2003). SsCVNH and BcCVNH were found to be highly conserved in both the DNA and the protein sequences, as confirmed by BlastN and BlastP searches on the National Center for Biotechnology Information (https://www.ncbi.nlm.nih.gov/). Deleting *SsCVNH* resulted in lower virulence and caused smaller lesion area than the wild-type strain on detached oilseed rape leaves and *Arabidopsis* leaves (Figure 1). We confirmed that *SsCVNH* plays an important role in virulence. In addition, the heterologous expression of *SsCVNH* in *A. thaliana* inhibited the PTI response and increased susceptibility, further demonstrating the significant role of effectors in the pathogenesis of *S. sclerotiorum* (Figure 3).

ROS act as a signalling molecules that sense and integrate various environmental signals and finally activate stress-response signalling networks to defend against a number of biotic and abiotic stresses (Mittler et al., 2022; Waszczak et al., 2018). Suppression of ROS production eventually leads to the inhibition of the plant immune response and exhibition of susceptibility (Kimura et al., 2020; Li et al., 2022). Nevertheless, excessive accumulation of ROS has detrimental effects on plant growth and development, leading to plant cell death and autophagy (Smirnoff & Arnaud, 2019). All in all, ROS are a double-edged sword, and the homeostasis of ROS, crucial to plant life cycle, is mainly maintained through ROS production, scavengers and transport (Mittler, 2017; Mittler et al., 2004, 2011). AtPRX71 is a class III peroxidase, which is a highly complex group of enzymes secreted into the extracellular space, vacuole and cell wall in *Arabidopsis*

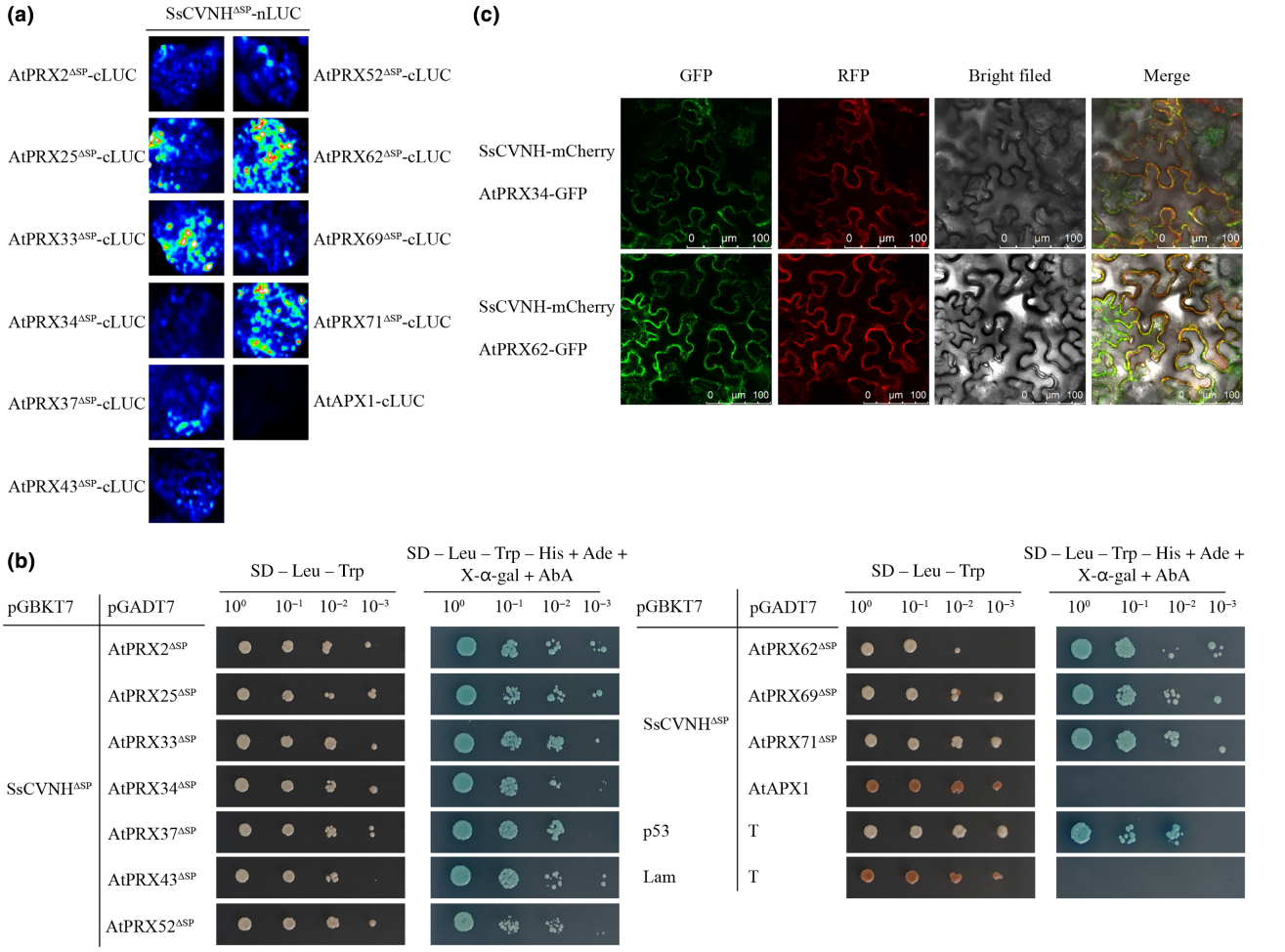

FIGURE 7 SsCVNH interacted with the class III peroxidase family of *Arabidopsis thaliana*. (a) Luciferase complementation assay confirmed the interaction of SsCVNH with AtPRXs after co-expressing SsCVNH$^{\Delta SP}$-nLUC and AtPRXs$^{\Delta SP}$-cLUC in the *Nicotiana benthamiana* epidermal cells. The leaves were treated 2 days later with substrate luciferin for 5 min, and chemiluminescence intensity was detected by the imaging system. SsCVNH$^{\Delta SP}$-nLUC and AtAPX1-cLUC were co-expressed as negative control. (b) Yeast two-hybrid assays showing that SsCVNH interacted with the class III peroxidase AtPRXs. SsCVNH$^{\Delta SP}$ was fused with the GAL4 binding domain (BD), and AtPRXs$^{\Delta SP}$ was fused with the GAL4 activation domain (AD). pGBKT7-p53 and pGADT7-T were co-expressed as positive control; pGBKT7-Lam and pGADT7-T were co-expressed as negative control; pGBKT7-SsCVNH$^{\Delta SP}$ and pGADT7-AtAPX1 were also co-expressed as negative control. (c) Co-expressing SsCVNH-mCherry with AtPRX34-GFP or AtPRX62-GFP in the *N. benthamiana* epidermal cells; the photographs were taken 3 days after agroinfiltration using confocal laser scanning microscopy. Scale bars =100 μm.

(Raggi et al., 2015). Some of them also function in the peroxisome. In *Arabidopsis* stems, AtPRX71 is distributed in the cell wall (Hoffmann et al., 2020). However, we confirmed that AtPRX71 is located in the cell membrane and extracellular space by transiently expressing *AtPRX71* in *N. benthamiana* leaves (Figure S6). This result demonstrates that AtPRX71 may have different localizations in different plant tissues. SsCVNH was confirmed to localize in plant cell membranes (Figure 5a), and SsCVNH was also detected in the apoplast fluid (Figure 5b). These results further confirmed the interaction between SsCVNH and AtPRX71 in cell membranes and apoplast (Figure 5).

Chitin-induced ROS bursts were significantly increased in *AtPRX71*-overexpressing plants and, conversely, were significantly decreased in *Atprx71* mutant plants. Although chitin-induced callose deposition and the resistance to *S. sclerotiorum* were higher in *AtPRX71*-overexpressing plants than in the wild-type plants, there was no obvious change in the *Atprx71* mutant (Figure 6). Previous studies have shown that the susceptibility of *Atprx71* mutant to *Botrytis cinerea* did not change either. This may be related to the redundant activity of these peroxidases (Raggi et al., 2015). For example, *Atprx33* and *Atprx34* also play important roles in plant disease resistance. Treatment of *Atprx33* and *Atprx34* knockdown lines with various PAMPs results in decreased ROS levels, enhanced susceptibility and reduced callose deposits (Daudi et al., 2012; Zhao et al., 2019).

These results led us to examine whether SsCVNH could also target other peroxidases. Subsequently, we found that SsCVNH did target members of the class III peroxidases family, including AtPRX2, AtPRX25, AtPRX33, AtPRX34, AtPRX52, AtPRX62 and AtPRX69 (Figure 7a,b). Aside from AtPRX71, AtPRX34 and AtPRX62 could also co-localize with SsCVNH in the cell membrane and apoplast

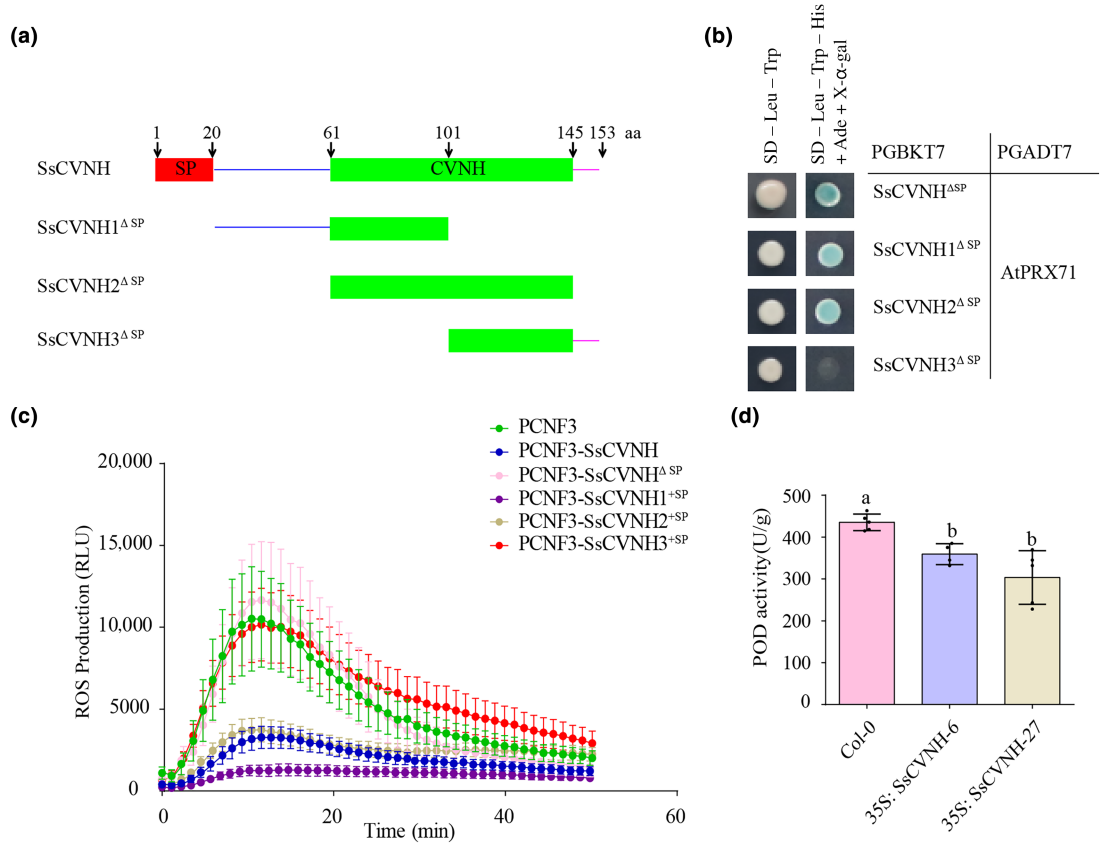

FIGURE 8 SsCVNH inhibits reactive oxygen species (ROS) burst through interaction with AtPRX71. (a) Schematic presentation of truncated SsCVNH for examination of its interaction with AtPRX71. Red square: signal peptide (SP), 1–20 amino acids (aa); blue line: 21–61 aa; green square: all or part CVNH domain; and magenta line, 145–153 aa. (b) Yeast two-hybrid confirmed that AtPRX71 could interact with SsCVNH1 and SsCVNH2 but not with SsCVNH3. (c) Empty vector PCNF3, full-length SsCVNH, SsCVNH without signal peptide and SsCVNH1, SsCVNH2 and SsCVNH3 with signal peptide were transiently expressed in 5-week-old *N. benthamiana* to examine the ROS burst. *Nicotiana benthamiana* leaf discs were treated with 200 nM chitin. The relative light units (RLUs) were measured. Values represent means ± *SEM* ($n = 16$). (d) The peroxidase activity of 35S:*SsCVNH-6*, 35S:*SsCVNH-27* transgenic plants and wild-type Col-0 plants 12 h after inoculation with wild-type 1980 detected with peroxidase (POD) activity test kit. Different lowercase letters above bars indicate significant difference.

(Figure 7c). We further confirmed that SsCVNH interacted with both AtPRX62 and AtPRX71 through Co-IP experiment (Figure 4d). These results can explain why *SsCVNH* transgenic plants are susceptible to *S. sclerotiorum* whereas the susceptibility of *Atprx71* mutant plants has not changed. RBOHD, which has six conserved transmembrane helices and intracellular cytosolic N- and C-termini, is the core member of RBOH family that produces ROS and responds to external stimuli (Lee et al., 2020). We found that neither the N-terminus nor the C-terminus of RBOHD interacted with SsCVNH$^{\Delta SP}$ (Figure S7). This suggests that the effect of SsCVNH on ROS homeostasis is not related to RBOHD.

According to the subcellular localization and origins of class I and class II peroxidases, we can speculate that SsCVNH would not target these two classes of peroxidases. Our Y2H assay results showed that class I peroxidase APX1, TAPX and APX3 did not interact with SsCVNH (Figure S7). Therefore, we concluded that SsCVNH might be able to only target members of the class III peroxidase family.

In summary, we have proposed a working model in which secreted virulence effectors, such as SsCVNH, inhibit the production of ROS by targeting class III peroxidases to enhance pathogen infection and increase host susceptibility. To our knowledge, SsCVNH is the first effector found in *S. sclerotiorum* that targets class III peroxidase to inhibit the host's immune response, thereby promoting *S. sclerotiorum* infection and colonization. Our results enhance our understanding of ROS in plant resistance to *S. sclerotiorum*. Furthermore, they broaden our knowledge of the pathogenesis of *S. sclerotiorum* and offer new insights for developing strategies to prevent and manage *Sclerotinia* diseases.

4 | EXPERIMENTAL PROCEDURES

4.1 | Fungal strains, plant lines and culture conditions

In this article, *S. sclerotiorum* wild-type strain 1980 was used and cultured on potato dextrose agar (PDA) or SY medium (5 g sucrose, 0.5 g yeast extract and 15 g agar per L) at 20°C. Knockout mutants were cultured on PDA with 50 μg/mL hygromycin B, and corresponding complemented mutants were cultured on PDA with 100 μg/mL

neomycin. Bacterial strains were cultured on Luria–Bertani (LB) medium at 37°C, and *A. tumefaciens* EHA105 and GV3101 were cultured on LB medium at 28°C.

Arabidopsis Col-0 was planted on half-strength Murashige and Skoog (MS) medium with 50 μg/mL cefotaxime at 4°C about 3 days and then transferred into the greenhouse about 8 days in which the temperature was 20°C under a 14-h light/10-h dark photoperiod and at 70%–80% relative humidity. Subsequently, the seedlings were transferred to the soil in the greenhouse. *AtPrx71* mutant (SALK_061054C) was bought from the ABRC (Arabidopsis Biological Resource Center). Transgenic lines 35S:*SsCVNH-6* and 35S:*SsCVNH*-27 were generated and treated as mentioned with 50 μg/mL kanamycin. 35S:*AtPRX71-7*- and 35S:*AtPRX71-9*-overexpressing plants were screened by selection with Basta. Four- to five-week-old leaves were used for ROS production, callose deposition and pathogen infection assays. The overexpressing plants in this study were in the Col-0 background. The wild-type *N. benthamiana* was planted in soil and placed in 9 cm square pots in the greenhouse at 28°C. Four to five weeks later, *N. benthamiana* plants were used to conduct the experiment. From the bottom to the top, the third to sixth leaves were used for co-expression experiments.

4.2 | Plasmid constructs for transient expression or overexpression in plants

S. sclerotiorum 1980 was inoculated on cellophane placed on PDA for 48 h, and then, mycelia were collected for RNA isolation by TRIzol reagent (Shachuan Biology). The EasyScript One-Step gDNA Removal and cDNA Synthesis SuperMix kit (Transgen Biotech) was used to synthesize cDNA, and then the *SsCVNH* coding sequence was PCR-amplified from cDNA. After digesting with enzymes, the amplified fragments were cloned into digested vector. All primers used in this study are listed in Table S2. The SsCVNH fragment was subcloned into the pCNF3 vector to generate 35S:*SsCVNH* transgenic lines. Col-0 cDNA was obtained from the leaf tissue of *A. thaliana* Col-0 plants grown for 4 weeks in soil in the greenhouse at 20°C by the same method as that of *S. sclerotiorum*. *AtPRX71* was amplified from Col-0 cDNA and then subcloned into TF101-GFP vector to generate 35S:*AtPRX71*-overexpressing plants.

4.3 | Gene replacement and complementation

The method of split-marker recombination was used to knock out *SsCVNH* (Catlett et al., 2003). The schematic diagram of the gene deletion strategy is illustrated in Figure S1a. The hygromycin resistance gene sequence was used to replace *SsCVNH* sequence that was amplified from 1980 genomic DNA. The hygromycin resistance gene sequence was split into HY and YG. The upstream sequence of about 1000 bp of *SsCVNH* and HY was fused by fusion PCR. The fused fragment named UHY was linked into the pMD18-T vector and transformed into *Escherichia coli*. The downstream sequence of about 1000 bp of *SsCVNH* and YG was fused by PCR. The fused fragment named YGD was linked into the pMD18-T vector and then transformed into *E. coli*.

Protoplasts of wild-type strain 1980 were prepared according to the method reported by Rollins (2003). Lysing enzyme from *Trichoderma harzianum* (1%; Sigma) was used to prepare protoplasts that were finally resuspended in STC solution (1 M sorbitol, 50 mM Tris–HCl, pH 8.0, 50 mM $CaCl_2$). The concentration of protoplasts was at least 10^8 protoplasts/mL.

At least 5 μg of the UHY and YGD fragments were mixed with protoplasts and incubated on ice for 30 min. One millilitre of protoplast transformation buffer was added into the mixture, and then the mixture was incubated at room temperature for 30 min. Finally, the mixture was dropped onto RM medium evenly without antibiotics. After the dish was placed at 12–16 h, RM medium with 100 μg/mL hygromycin was covered in the RM dish. PDA plates with 100 μg/mL hygromycin were used to screen the potential mutants. PCR was carried out to detect the potential mutants.

To induce apothecium production, a large number of sclerotia of Δ*SsCVNH* were collected. The sclerotia were kept at 4°C for 2 weeks and then transferred to 20°C with high humidity and low light. After about 45 days, the sclerotia germinated to form apothecia. The apothecia were placed in a 10-mL syringe filled with water, and the liquid was dispensed onto the PDA plate containing hygromycin after pushing and pulling the syringe more than 30 times. The mycelium growing on the PDA plate was the candidate homozygous knockout mutant. Homokaryotic Δ*SsCVNH* knockout mutants were further identified by PCR with four primer pairs (PF1/PR1, HYG-F/HYG-R, PF3/PR3 and CVNH-F/CVNH-R) and Southern blot.

For gene complementation assay, 1980 strain genomic DNA was used as a template to amplify the *SsCVNH* sequence including the promoter region. The *SsCVNH* sequence was subcloned into the pCETNS-4 vector. The expression vector was transformed into *A. tumefaciens* EHA105, which was used to transform the deletion mutants using the ATMT method (Yu et al., 2012).

4.4 | RNA extraction and quantitative real-time PCR

The total RNA of fungi and plants was isolated with TRIzol. The first-strand cDNA was synthesized by M-MLV reverse transcriptase at 42°C for 30 min. SYBR Green Supermix (2×) was used for quantitative real-time PCR (qPCR) analysis in a CFX96 Real-Time PCR Detection System (Bio-Rad) with specific primers, which are listed in Table S2. The *S. sclerotiorum* gene *Sstub1* (SS1G_04652) was used as reference in the reverse transcription (RT)-qPCR (Figure S1d). *Arabidopsis* gene *GAPDH* (AT1G13440) was used as a housekeeping gene to normalize the expression of the genes of interest. *FRK1* and *NHL10* are early immune-related genes; 0, 30 and 60 min samples were selected for the RT-qPCR experiment (Li et al., 2019). *GST6* and *PR1* are late immune-related genes; 0, 1 and 3 h samples were selected for the RT-qPCR experiment (Mammarella et al., 2015).

4.5 | Pathogenicity assays

S. sclerotiorum 1980 strains and mutants from a 4°C slant were inoculated onto PDA at 20°C for 36 h and then inoculated onto 2×SY medium for 48 h. Five-week-old *Arabidopsis* plants were used to conduct pathogenicity assays, and more than 10 true leaves were inoculated with agar plugs (3 mm diameter) from the edge of rapidly growing mycelium on 2×SY medium. About seven *B. napus* leaves were inoculated with agar plugs (5 mm diameter) from the edge of rapidly growing mycelium on 2×SY medium. The disease symptoms were photographed, and necrotic lesions were measured 24 or 36 h post-inoculation.

4.6 | *Agrobacterium*-mediated transient expression in *N. benthamiana* and generation of transgenic *Arabidopsis* lines

BamHI-digested SsCVNH and SsCVNH$^{\Delta SP}$ were cloned into BamHI-digested pCNG9 vector to construct pCNF3-SsCVNH-GFP and pCNF3-SsCVNH$^{\Delta SP}$–GFP, respectively. *A. tumefaciens* GV3101 containing above plasmids was infiltrated into *N. benthamiana* leaves on the lower epidermal side. After 48 h, a confocal laser scanning microscope (LAS SP 8.0) was used to observe fluorescence. BamHI/SmaI-digested SsCVNH was cloned into BamHI/SmaI-digested pCNF3 vector to construct the 2×35S:SsCVNH-FLAG vector. XbaI/StuI-digested AtPRX71 was cloned into XbaI/StuI-digested TF101-GFP vector to construct the 2×35S:*AtPRX71*-GFP vector. For overexpressing lines, Col-0 was transformed with 2×35S:*SsCVNH*-FLAG or 2×35S:*AtPRX71*-GFP, generating *SsCVNH* or *AtPRX71* transgene lines. The *A. tumefaciens* GV3101 containing the above plasmids was suspended in 5% sucrose solution containing 0.02% Silwet L-77. The inflorescences of *Arabidopsis* were immersed in suspension solution as described above. After 16-h dark culture, plants were transferred into the greenhouse.

4.7 | Screening of *Arabidopsis* cDNA library and Y2H assay

S. sclerotiorum 1980 was grown on PDA plates for 48 h. Mycelium agar plugs were taken by using a 3-mm puncher and then inoculated onto 4-week-old *A. thaliana* Col-0 plants. The leaves were collected at 0, 1, 3, 6, 12 and 24 h to construct an *Arabidopsis* cDNA library by OE Biotech (Shanghai) via cloning the full-length open reading frames that consisted of the entire *Arabidopsis* genes into the pGADT7 vector.

Before screening the *Arabidopsis* cDNA library, a self-activation verification assay was conducted. SsCVNH$^{\Delta SP}$-pGBKT7 vector was constructed and transformed into Y2HGold strain followed by dropping into the SD−Trp+X-α-gal + aureobasidin A (AbA) medium. pGBKT7 vector acted as a control.

SsCVNH$^{\Delta SP}$ Y2HGold strain acted as bait and *Arabidopsis* cDNA library acted as prey; bait and prey were mated in 2×YPD liquid medium at 30°C for 20–24 h. Finally, 0.5×YPD was used to resuspend cells, which were dropped onto SD − Trp − Leu − His + X-α-gal + AbA medium plates. Blue spots of SD − Trp − Leu − His + X-α-gal + AbA plates were sequenced and verified by Y2H with *SsCVNH*.

SsCVNH$^{\Delta SP}$ and AtPRX71 combined with different domains in pGPKT7 and pGADT7 vector were co-transformed into Y2H strain. Polyethylene glycol/lithium acetate and carrier DNA were used according to the protocol (http://www.weidibio.com/display.php?id=339). Finally, co-transformed yeast strains were cultured on SD − Trp − Leu − His − Ade+X-α-gal + AbA medium to confirm the protein–protein interaction.

4.8 | Luminol-based ROS assays in *A. thaliana*

Leaves of 4-week-old *Arabidopsis* plants were punched into leaf discs of 0.25 cm^2 and cut into four strips. To eliminate the wounding effect, leaf discs were incubated overnight in 96-well plates with 100 μL double-distilled water. The measurement parameter (one cycle of about 1.5 min, 45 cycles) was set up (Li et al., 2019). Before detection, double-distilled water was removed and replaced with a 100 μL mixture reaction solution containing 50 μM luminol (Sigma), 10 μg/mL horseradish peroxidase (Sigma) and 200 nM chitin. The 96-well plate was placed into the microplate reader, and the measurement was carried out immediately. The values of ROS production are represented by the relative light units (RLU) of different lines.

4.9 | Callose deposition assay

Five-week-old *Arabidopsis* leaves were infiltrated with water or chitin and cultured normally for 24 h. The leaves were transferred into 12-well plates with FAA solution (10% formaldehyde, 5% acetic acid and 50% ethanol) to incubate for 12 h and were destained in 95% ethanol for 6 h to make the leaves transparent. Next, the leaves were washed with 70% ethanol and double-distilled water, and then the leaves were dipped in 0.01% aniline blue solution (150 mM KH_2PO_4, pH 9.5) for 30 min. The stained leaves were fixed on the slide with 50% glycerol. Callose deposition was observed by fluorescence microscope, and the image was processed by ImageJ v. 1.0.

4.10 | Co-IP assay

SsCVNH-PCNF3, AtPRX62-TF101-GFP, AtPRX71-TF101-GFP and TF101-GFP vectors were transformed into *A. tumefaciens* GV3101 by electroporation. The OD_{600} was adjusted to 1.5 before infiltration. After 2 days, five leaf discs were collected into a tube, and then, 200 μL Co-IP buffer (20 mM Tris–HCl, pH 7.5, 100 mM NaCl, 1 mM EDTA, 2 mM dithiothreitol, 10% glycerol, 0.5% Triton

X-100 and protease inhibitor) was added into tube after grinding the samples on ice for 30 min. Five-microlitre samples (GFP Trap) were added into the supernatant, and the mixture was incubated at 4°C for 1–3 h in a turning mixer. At last, the mixture was washed with Co-IP washing buffer (20 mM Tris–HCl, pH 7.5, 100 mM NaCl, 1 mM EDTA and 0.1% Triton X-100) five times. The immunoprecipitated (IP) protein and the input protein were analysed by immunoblotting with an anti-FLAG antibody and anti-GFP antibody (Promoter Biological Company).

4.11 | Bimolecular fluorescence complementation assay

AtPRX71-cRFP, SsCVNH-nRFP, cRFP and nRFP vectors were constructed and introduced into *A. tumefaciens* GV3101 by electroporation. AtPRX71-cRFP and SsCVNH-nRFP were co-expressed in *N. benthamiana* to observe the red fluorescence. The AtPRX71-cRFP and nRFP or cRFP and SsCVNH-nRFP were co-expressed as controls. After 2 days, the RFP fluorescence was observed using confocal microscopy.

4.12 | Protein production and peroxidase activity assays

Plant leaves (5 weeks old) were inoculated with *S. sclerotiorum* 1980. Twelve hours later, 0.1 g leaf samples were collected and ground into a powder. Phosphate buffer (1 M, pH 7.5) was added to prepare 10% tissue homogenate. According to the peroxidase (POD) test kit, the POD activity was detected by measuring the absorbance change at 420 nm (Nanjing Jiancheng Bioengineer Institute).

ACKNOWLEDGEMENTS

The study was supported by the National Nature Science Foundation of China (31701735, 32172368 and 32130087), the earmarked fund of China Agriculture Research System (CARS-12) and the Huazhong Agricultural University Scientific and Technological Self-innovation Foundation (2021ZKPY014).

DATA AVAILABILITY STATEMENT

The data that support the findings of this study are available from the corresponding author upon reasonable request.

ORCID

Bo Li https://orcid.org/0000-0002-7337-0112
Tao Chen https://orcid.org/0000-0003-4614-4440
Yang Lin https://orcid.org/0000-0003-3942-7063
Jiasen Cheng https://orcid.org/0000-0003-0040-2360

REFERENCES

Adams, P.B. & Ayers, W.A. (1979) Ecology of *Sclerotinia* species. *Phytopathology*, 69, 896–899.

Amselem, J., Cuomo, C.A., van Kan, J.A.L., Viaud, M., Benito, E.P., Couloux, A. et al. (2011) Genomic analysis of the necrotrophic fungal pathogens *Sclerotinia sclerotiorum* and *Botrytis cinerea*. *PLoS Genetics*, 7, e1002230.

Ausubel, F.M. (2005) Are innate immune signaling pathways in plants and animals conserved? *Nature Immunology*, 6, 973–979.

Bakalovic, N., Passardi, F., Ioannidis, V., Cosio, C., Penel, C., Falquet, L. et al. (2006) PeroxiBase: a class III plant peroxidase database. *Phytochemistry*, 67, 534–539.

Barrientos, L.G., Louis, J.M., Ratner, D.M., Seeberger, P.H. & Gronenborn, A.M. (2003) Solution structure of a circular-permuted variant of the potent HIV-inactivating protein cyanovirin-N: structural basis for protein stability and oligosaccharide interaction. *Journal of Molecular Biology*, 325, 211–223.

Boland, G.J. & Hall, R. (1994) Index of plant hosts of *Sclerotinia sclerotiorum*. *Canadian Journal of Plant Pathology*, 16, 93–108.

Boller, T. & Felix, G. (2009) A renaissance of elicitors: perception of microbe-associated molecular patterns and danger signals by pattern-recognition receptors. *Annual Review of Plant Biology*, 60, 379–406.

Bolton, M.D., Thomma, B.P. & Nelson, B.D. (2006) *Sclerotinia sclerotiorum* (Lib.) de Bary: biology and molecular traits of a cosmopolitan pathogen. *Molecular Plant Pathology*, 7, 1–16.

Boutrot, F. & Zipfel, C. (2017) Function, discovery, and exploitation of plant pattern recognition receptors for broad-spectrum disease resistance. *Annual Review of Phytopathology*, 55, 257–286.

Catlett, N.L., Lee, B.N., Yoder, O.C. & Turgeon, B.G. (2003) Split-marker recombination for efficient targeted deletion of fungal genes. *Fungal Genetics Reports*, 50, 9–11.

Clarkson, J.P., Phelps, K., Whipps, J.M., Young, C.S., Smith, J.A. & Watling, M. (2007) Forecasting sclerotinia disease on lettuce: a predictive model for carpogenic germination of *Sclerotinia sclerotiorum* sclerotia. *Phytopathology*, 97, 621–632.

Cosio, C. & Dunand, C. (2009) Specific functions of individual class III peroxidase genes. *Journal of Experimental Botany*, 60, 391–408.

Couto, D. & Zipfel, C. (2016) Regulation of pattern recognition receptor signalling in plants. *Nature Reviews Immunology*, 16, 537–552.

Daudi, A., Cheng, Z., O'Brien, J.A., Mammarella, N., Khan, S., Ausubel, F.M. et al. (2012) The apoplastic oxidative burst peroxidase in *Arabidopsis* is a major component of pattern-triggered immunity. *The Plant Cell*, 24, 275–287.

Derbyshire, M.C., Newman, T.E., Khentry, Y. & Taiwo, A.O. (2022) The evolutionary and molecular features of the broad-host-range plant pathogen *Sclerotinia sclerotiorum*. *Molecular Plant Pathology*, 23, 1075–1090.

Ding, Y.J., Mei, J.J., Chai, Y., Yang, W.J., Mao, Y., Yan, B.Q. et al. (2020) *Sclerotinia sclerotiorum* utilizes host-derived copper for ROS detoxification and infection. *PLoS Pathogens*, 16, e1008919.

Duan, Y., Xiu, Q., Li, H., Li, T., Wang, J. & Zhou, M.G. (2019) Pharmacological characteristics and control efficacy of a novel SDHI fungicide pydiflumetofen against *Sclerotinia sclerotiorum*. *Plant Disease*, 103, 77–82.

Duan, Y.B., Li, T., Xiao, X.M., Wu, J., Li, S.K., Wang, J.X. et al. (2018) Pharmacological characteristics of the novel fungicide pyrisoxazole against *Sclerotinia sclerotiorum*. *Pesticide Biochemistry and Physiology*, 149, 61–66.

Fan, H., Yang, W., Nie, J., Zhang, W., Wu, J., Wu, D. et al. (2021) A novel effector protein SsERP1 inhibits plant ethylene signaling to promote *Sclerotinia sclerotiorum* infection. *Journal of Fungi*, 7, 825–839.

Gara, L.D. (2004) Class III peroxidases and ascorbate metabolism in plants. *Phytochemistry Reviews*, 3, 195–205.

Godoy, G., Steadman, J.R., Dickman, M.B. & Dam, R. (1990) Use of mutants to demonstrate the role of oxalic acid in pathogenicity of *Sclerotinia sclerotiorum* on *Phaseolus vulgaris*. *Physiological and Molecular Plant Pathology*, 37, 179–191.

Gómez-Gómez, L. & Boller, T. (2000) FLS2: an LRR receptor–like kinase involved in the perception of the bacterial elicitor flagellin in *Arabidopsis*. *Molecular Cell*, 5, 1003–1011.

Gupta, N.C., Yadav, S., Arora, S., Mishra, D.C., Budhlakoti, N., Gaikwad, K. et al. (2022) Draft genome sequencing and secretome profiling of *Sclerotinia sclerotiorum* revealed effector repertoire diversity and allied broad-host range necrotrophy. *Scientific Reports*, 12, 21855.

Guyon, K., Balagué, C., Roby, D. & Raffaele, S. (2014) Secretome analysis reveals effector candidates associated with broad host range necrotrophy in the fungal plant pathogen *Sclerotinia sclerotiorum*. *BMC Genomics*, 15, 336.

Hiraga, S., Sasaki, K., Ito, H., Ohashi, Y. & Matsui, H. (2001) A large family of class III plant peroxidases. *Plant and Cell Physiology*, 42, 462–468.

Hoffmann, N., Benske, A., Betz, H., Schuetz, M. & Samuels, A.L. (2020) Laccases and peroxidases co-localize in lignified secondary cell walls throughout stem development. *Plant Physiology*, 184, 806–822.

Jia, L.G., Xu, W.F., Li, W.R., Ye, N.H., Liu, R., Shi, L. et al. (2013) Class III peroxidases are activated in proanthocyanidin-deficient *Arabidopsis thaliana* seeds. *Annals of Botany*, 111, 839–847.

Jones, J.D. & Dangl, J.L. (2006) The plant immune system. *Nature*, 444, 323–329.

Kabbage, M., Williams, B. & Dickman, M.B. (2013) Cell death control: the interplay of apoptosis and autophagy in the pathogenicity of *Sclerotinia sclerotiorum*. *PLoS Pathogens*, 9, e1003287.

Kabbage, M., Yarden, O. & Dickman, M.B. (2015) Pathogenic attributes of *Sclerotinia sclerotiorum*: switching from a biotrophic to necrotrophic lifestyle. *Plant Science*, 233, 53–60.

Kim, K.S., Min, J.Y. & Dickman, M.B. (2008) Oxalic acid is an elicitor of plant programmed cell death during *Sclerotinia sclerotiorum* disease development. *Molecular Plant–Microbe Interactions*, 21, 605–612.

Kimura, S., Hunter, K., Vaahtera, L., Tran, H.C., Citterico, M., Vaattovaara, A. et al. (2020) CRK2 and C-terminal phosphorylation of NADPH oxidase RBOHD regulate reactive oxygen species production in *Arabidopsis*. *The Plant Cell*, 32, 1063–1080.

Lee, D., Lal, N.K., Lin, Z.D., Ma, S., Liu, J., Castro, B. et al. (2020) Regulation of reactive oxygen species during plant immunity through phosphorylation and ubiquitination of RBOHD. *Nature Communications*, 11, 1838.

Li, B., Ferreira, M.A., Huang, M., Camargos, L.F., Yu, X., Teixeira, R.M. et al. (2019) The receptor-like kinase NIK1 targets FLS2/BAK1 immune complex and inversely modulates antiviral and antibacterial immunity. *Nature Communications*, 10, 4996.

Li, G.B., He, J.X., Wu, J.L., Wang, H., Zhang, X., Liu, J. et al. (2022) Overproduction of OsRACK1A, an effector-targeted scaffold protein promoting OsRBOHB-mediated ROS production, confers rice floral resistance to false smut disease without yield penalty. *Molecular Plant*, 15, 1790–1806.

Li, W.T., Zhu, Z.W., Chern, M.S., Yin, J.J., Yang, C., Ran, L. et al. (2017) A natural allele of a transcription factor in rice confers broad-spectrum blast resistance. *Cell*, 170, 114–126.

Liang, X.F. & Rollins, J.A. (2018) Mechanisms of broad host range necrotrophic pathogenesis in *Sclerotinia sclerotiorum*. *Phytopathology*, 108, 1128–1140.

Liu, H., Dong, S.Y., Li, M., Gu, F.W., Yang, G.L., Guo, T. et al. (2020) The class III peroxidase gene *OsPrx30*, transcriptionally modulated by the AT-hook protein OsATH1, mediates rice bacterial blight-induced ROS accumulation. *Journal of Integrative Plant Biology*, 63, 393–408.

Lorrai, R., Francocci, F., Gully, K., Martens, H.J., De Lorenzo, G., Nawrath, C. et al. (2021) Impaired cuticle functionality and robust resistance to *Botrytis cinerea* in *Arabidopsis thaliana* plants with altered homogalacturonan integrity are dependent on the class III peroxidase AtPRX71. *Frontiers in Plant Science*, 12, 696955.

Lyu, X.L., Shen, C.C., Fu, Y.P., Xie, J.T., Jiang, D.H., Li, G. et al. (2015) Comparative genomic and transcriptional analyses of the carbohydrate-active enzymes and secretomes of phytopathogenic fungi reveal their significant roles during infection and development. *Scientific Reports*, 5, 15565.

Lyu, X.L., Shen, C.C., Fu, Y.P., Xie, J.T., Jiang, D.H., Li, G. et al. (2016) A small secreted virulence-related protein is essential for the necrotrophic interactions of *Sclerotinia sclerotiorum* with its host plants. *PLoS Pathogens*, 12, e1005435.

Macho, A.P. & Zipfel, C. (2014) Plant PRRs and the activation of innate immune signaling. *Molecular Cell*, 54, 263–272.

Mammarella, N.D., Cheng, Z.Y., Fu, Z.Q., Daudi, A., Bolwell, G.P., Dong, X.N. et al. (2015) Apoplastic peroxidases are required for salicylic acid-mediated defense against *Pseudomonas syringae*. *Phytochemistry*, 112, 110–121.

Marolano, P., Dr Lenna, P. & Magro, P. (1983) Oxalic acid, cell wall-degrading enzymes and pH in pathogenesis and their significance in the virulence of two *Sclerotinia sclerotiorum* isolates on sunflower. *Physiological Plant Pathology*, 22, 339–345.

Mittler, R. (2017) ROS are good. *Trends in Plant Science*, 22, 11–19.

Mittler, R., Vanderauwera, S., Gollery, M. & Van Breusegem, F. (2004) Reactive oxygen gene network of plants. *Trends in Plant Science*, 9, 490–498.

Mittler, R., Vanderauwera, S., Suzuki, N., Miller, G., Tognetti, V.B., Vandepoele, K. et al. (2011) ROS signaling: the new wave? *Trends in Plant Science*, 16, 300–309.

Mittler, R., Zandalinas, S.I., Fichman, Y. & Breusegem, F.V. (2022) Reactive oxygen species signalling in plant stress responses. *Nature Reviews Molecular Cell Biology*, 23, 663–679.

Percudani, R., Montanini, B. & Ottonello, S. (2005) The anti-HIV cyanovirin-N domain is evolutionarily conserved and occurs as a protein module in eukaryotes. *Proteins: Structure, Function, and Bioinformatics*, 60, 670–678.

Peyraud, R., Mbengue, M., Barbacci, A. & Raffaele, S. (2019) Intercellular cooperation in a fungal plant pathogen facilitates host colonization. *Proceedings of the National Academy of Sciences of the United States of America*, 116, 3193–3201.

Purdy, L.H. (1979) *Sclerotinia sclerotiorum*—history, diseases and symptomatology, host range, geographic distribution, and impact. *Phytopathology*, 69, 875–880.

Qi, P.P., Huang, M.L., Hu, X.H., Zhang, Y., Wang, Y., Li, P.Y. et al. (2022) A *Ralstonia solanacearum* effector targets TGA transcription factors to subvert salicylic acid signaling. *The Plant Cell*, 34, 1666–1683.

Raggi, S., Ferrarini, A., Delledonne, M., Dunand, C., Ranocha, P., De Lorenzo, G. et al. (2015) The *Arabidopsis* class III peroxidase AtPRX71 negatively regulates growth under physiological conditions and in response to cell wall damage. *Plant Physiology*, 169, 2513–2525.

Rollins, J.A. (2003) The *Sclerotinia sclerotiorum pac1* gene is required for sclerotial development and virulence. *Molecular Plant–Microbe Interactions*, 16, 785–795.

Smirnoff, N. & Arnaud, D. (2019) Hydrogen peroxide metabolism and functions in plants. *New Phytologist*, 221, 1197–1214.

Tang, L.G., Yang, G.G., Ma, M., Liu, X.F., Li, B., Xie, J.T. et al. (2020) An effector of a necrotrophic fungal pathogen targets the calcium-sensing receptor in chloroplasts to inhibit host resistance. *Molecular Plant Pathology*, 21, 686–701.

Tao, X., Zhao, H.H., Xu, H.R., Li, Z.K., Wang, J.X., Song, X.S. et al. (2021) Antifungal activity and biological characteristics of the novel fungicide quinofumelin against *Sclerotinia sclerotiorum*. *Plant Disease*, 105, 2567–2574.

Teixeira, F.K., Menezes-Benavente, L., Margis, R. & Margis-Pinheiro, M. (2004) Analysis of the molecular evolutionary history of the ascorbate peroxidase gene family: inferences from the rice genome. *Journal of Molecular Evolution*, 59, 761–770.

Wang, P., Wang, Y.B., Hu, Y.W., Chen, Z.Y., Han, L.L., Zhu, W.J. et al. (2024) Plant hypersensitive induced reaction protein facilitates cell death induced by secreted xylanase associated with the pathogenicity of *Sclerotinia sclerotiorum*. *The Plant Journal*, 118, 90–105.

Waszczak, C., Carmody, M. & Kangasjarvi, J. (2018) Reactive oxygen species in plant signaling. *Annual Review of Plant Biology*, 69, 209–236.

Wei, W., Xu, L.S., Peng, H., Zhu, W.J., Tanaka, K., Cheng, J.S. et al. (2022) A fungal extracellular effector inactivates plant polygalacturonase-inhibiting protein. *Nature Communications*, 13, 2213.

Xiao, X.Q., Xie, J.T., Cheng, J.S., Li, G.Q., Yi, X., Jiang, D.H. et al. (2014) Novel secretory protein Ss-Caf1 of the plant-pathogenic fungus *Sclerotinia sclerotiorum* is required for host penetration and normal sclerotial development. *Molecular Plant–Microbe Interactions*, 27, 40–55.

Xu, L.S. & Chen, W.D. (2013) Random T-DNA mutagenesis identifies a Cu/Zn superoxide dismutase gene as a virulence factor of *Sclerotinia sclerotiorum*. *Molecular Plant–Microbe Interactions*, 26, 431–441.

Yang, C.H.Z., Li, W., Huang, X.C., Tang, X.Y., Qin, L., Liu, Y.N. et al. (2022) SsNEP2 contributes to the virulence of *Sclerotinia sclerotiorum*. *Pathogens*, 11, 446–459.

Yang, G.G., Tang, L.G., Gong, Y.D., Xie, J.T., Fu, Y.P., Jiang, D.H. et al. (2017) A cerato-platanin protein SsCP1 targets plant PR1 and contributes to virulence of *Sclerotinia sclerotiorum*. *New Phytologist*, 217, 739–755.

Yang, Y.k., Steidele, C.E., Rössner, C., Löffelhardt, B., Kolb, D., Leisen, T. et al. (2023) Convergent evolution of plant pattern recognition receptors sensing cysteine-rich patterns from three microbial kingdoms. *Nature Communications*, 14, 3621.

Yu, X., Feng, B., He, P. & Shan, L. (2017) From chaos to harmony: responses and signaling upon microbial pattern recognition. *Annual Review of Phytopathology*, 55, 109–137.

Yu, Y., Jiang, D.H., Xie, J.T., Cheng, J.S., Li, G.Q., Yi, X.H. et al. (2012) Ss-Sl2, a novel cell wall protein with PAN modules, is essential for sclerotial development and cellular integrity of *Sclerotinia sclerotiorum*. *PLoS ONE*, 7, e34962.

Zhao, J., Buchwaldt, L., Rimmer, S.R., Sharpe, A., McGregor, L., Bekkaoui, D. et al. (2009) Patterns of differential gene expression in *Brassica napus* cultivars infected with *Sclerotinia sclerotiorum*. *Molecular Plant Pathology*, 10, 635–649.

Zhao, L., Phuong, L.T., Luan, M.T., Fitrianti, A.N., Matsui, H., Nakagami, H. et al. (2019) A class III peroxidase PRX34 is a component of disease resistance in *Arabidopsis*. *Journal of General Plant Pathology*, 85, 405–412.

Zhu, W.J., Wei, W., Fu, Y.P., Cheng, J.S., Xie, J.T., Li, G.Q. et al. (2013) A secretory protein of necrotrophic fungus *Sclerotinia sclerotiorum* that suppresses host resistance. *PLoS One*, 8, e53901.

SUPPORTING INFORMATION

Additional supporting information can be found online in the Supporting Information section at the end of this article.

How to cite this article: Ma, M., Tang, L., Sun, R., Lyu, X., Xie, J., Fu, Y. et al. (2024) An effector SsCVNH promotes the virulence of *Sclerotinia sclerotiorum* through targeting class III peroxidase AtPRX71. *Molecular Plant Pathology*, 25, e13464. Available from: https://doi.org/10.1111/mpp.13464